Supplementary Information for

Resolution-enhanced X-ray Fluorescence Microscopy via Deep Residual Networks

Longlong Wu[1,2*], Seongmin Bak[3], Youngho Shin[4], Yong. S Chu[3], Shinjae Yoo[1], Ian K. Robinson[2,5†] and Xiaojing Huang[3‡]

[1]*Computational Science Initiative, Brookhaven National Laboratory, Upton, NY 11973, USA*

[2]*Condensed Matter Physics and Materials Science Department, Brookhaven National Laboratory, Upton, NY 11973, USA*

[3]*National Synchrotron Light Source II, Brookhaven National Laboratory, Upton, New York 11973, USA*

[4]*Materials Engineering Research Facility, Applied Materials Division, Argonne National Laboratory, Lemont, IL 60439, USA*

[5]*London Centre for Nanotechnology, University College London, London, WC1E 6BT, United Kingdom.*

[*]lwu@bnl.gov, [†]irobinson@bnl.gov, [‡]xjhuang@bnl.gov

Supplementary Figures

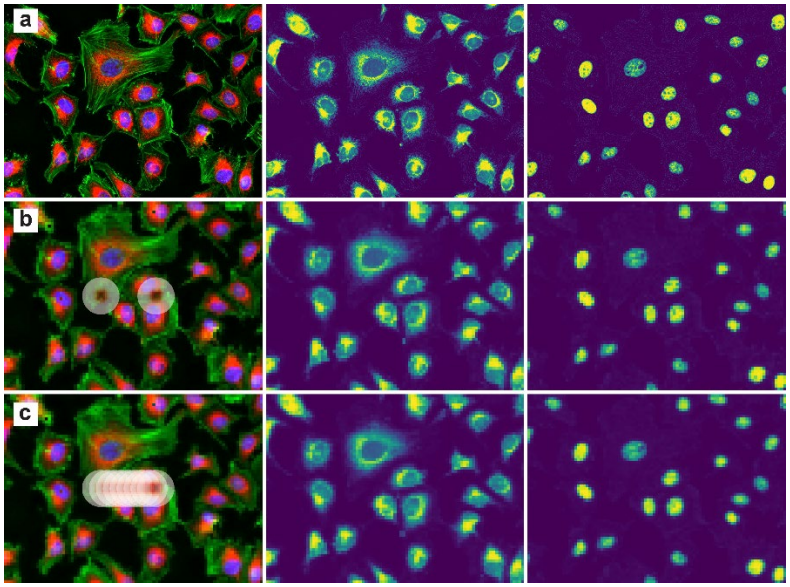

Supplementary Figure 1 | Representative illustration of the simulation of X-ray fluorescence (XRF) images for the RDN model with a focused X-ray beam. **a** Original combined high-resolution XRF images from different X-ray emission energy and corresponding energy-resolved XRF images. **b** Simulated low-resolution XRF images with a step scan mode and (**c**) with on-the-fly scan schemes. As shown above, different scanning methods will give different low-resolution XRF images when using the same high-resolution XRF image.

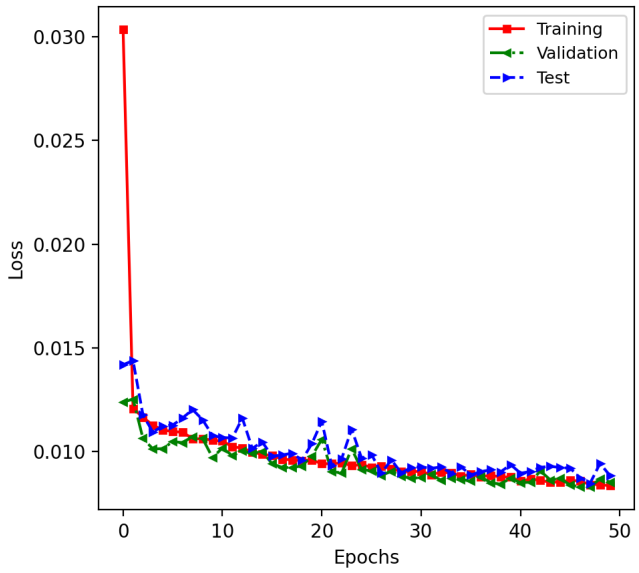

Supplementary Figure 2 | Training, validation, and test loss as a function of the training epochs for RDN model

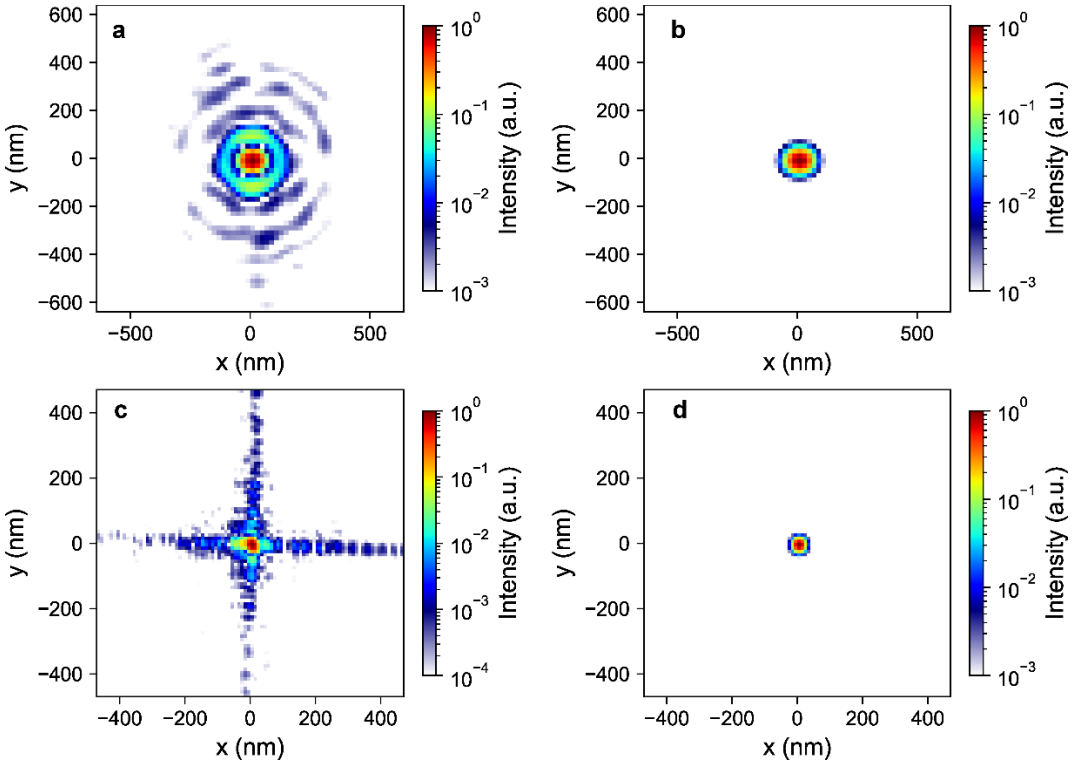

Supplementary Figure 3 | Estimation of X-ray beam sizes and resolutions for the scanning low-resolution XRF images. **a** X-ray beam from the Fresnel Zone Plate. **b** Corresponding result of a 2D fit of (**a**) to a Gaussian function. **c** X-ray beam from the Multilayer Laue Lenses (MLLs). **c** Corresponding results of a 2D fit of (**c**) to a Gaussian function. As the fitted result shown in (**b**) and (**d**), the calculated X-ray probe size for the FZP is 61.6 nm and 24.7 nm for the MLLs. For the directly obtained scanning XRF images, the X-ray beam information is convoluted with these XRF images. Therefore, considering the scanning step size as well as the X-ray beam size, the resolution of these low-resolution XRF images, the estimated resolution should be greater than the scanning step size. As shown in Supplementary Fig. 4a and 4b, using the Fourier shell correlation (FSC), the estimated for the directly obtained XRF images after the tomography reconstruction is 70 nm for the FZP and 50 nm for the MLLs. In these directly obtained XRF images, the X-ray probe profile is still convoluted with the sample information. Therefore, by further considering the X-ray probe size, the final resolution for these directly obtained XRF images can be estimated as $\sqrt{b^2 + s^2}$, where b is the X-ray probe size and s is the scanning step size (or the estimated resolution by using FSC). Finally, for the LR XRF image from the FZP, the corresponding resolution is $\sqrt{61.6^2 + 72.0^2} = 94.8$ nm and is $\sqrt{24.7^2 + 51.8^2} = 57.4$ nm from the MLLs.

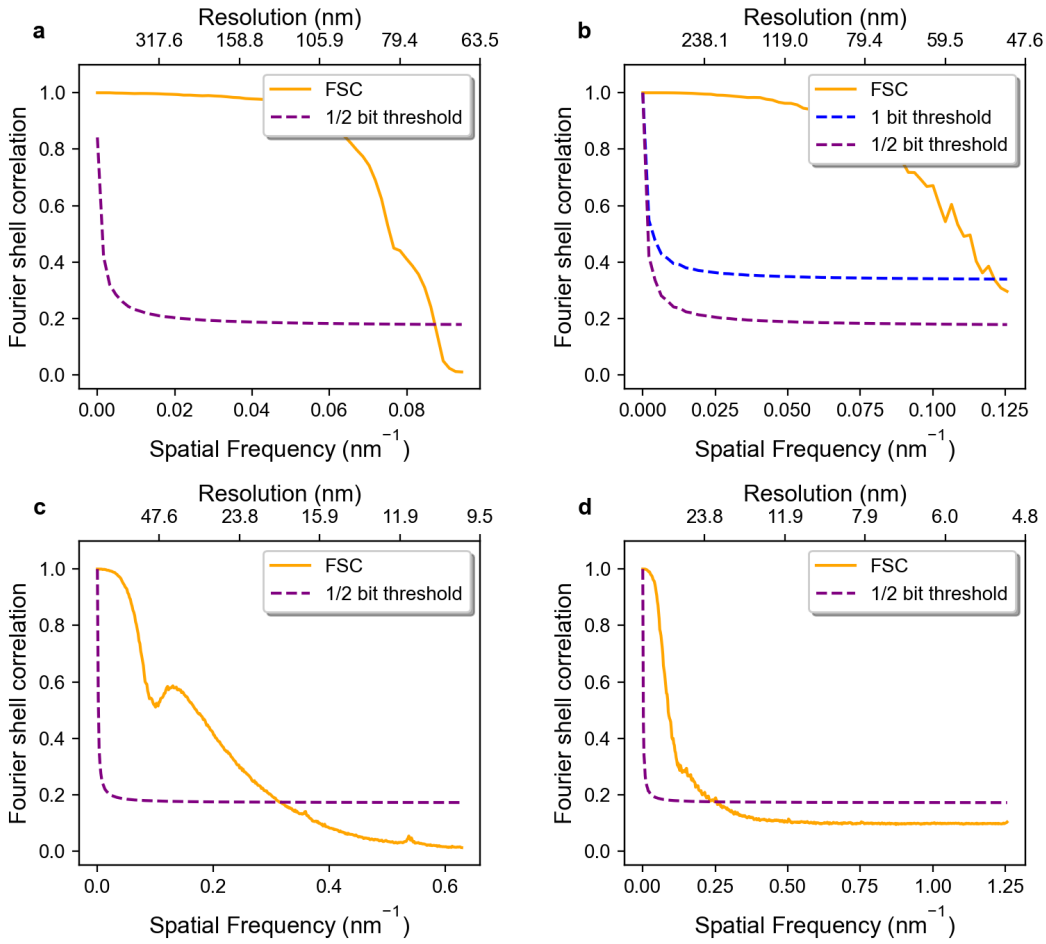

Supplementary Figure 4 | Resolution estimation for the volumes reconstructed XRF images after tomography reconstruction, obtained using two experimental datasets for each sample. **a** Fourier shell correlation (FSC) of the directly obtained XRF using a Fresnel Zone Plate (FZP). **b** FSC of the directly obtained XRF using a pair of Multilayer Laue lenses (MLLs). **c** Corresponding FSC of the obtained HR XRF images using the FZP. **d** Corresponding FSC of the obtained HR XRF images using MLLs. For the directly obtained XRF images, the resolution of 72.0 nm for the FZP using the half-bit threshold and 51.8 nm for the MLLs using the one-bit threshold were estimated, respectively. For the corresponding resolution-enhanced XRF images, the resolution of 22.0 nm for the FZP and 24.5 nm for the MLLs were estimated. See also Supplemental Fig. 6 for the corresponding Power Spectral Density.

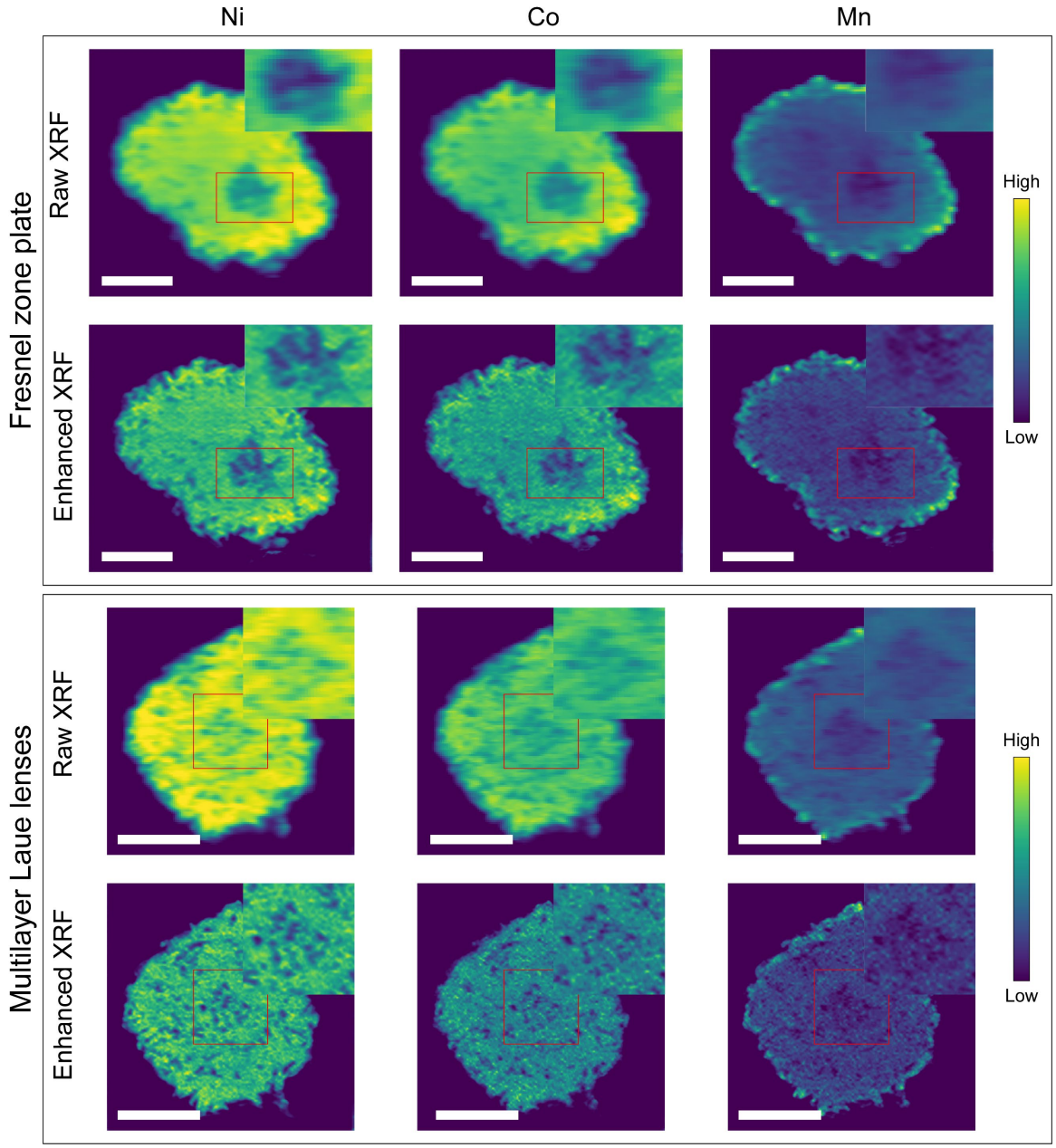

Supplementary Figure 5 | Comparison of experimental low- and high-resolution XRF images from different elements (i.e., Ni, Co, and Mo). Two different X-ray nanoprobes (i.e., FZP and MLLs) are used separately. In each image, the central slices of the 3D reconstructed structures of NMC particles are displayed. All the scale bars are 2 μm.

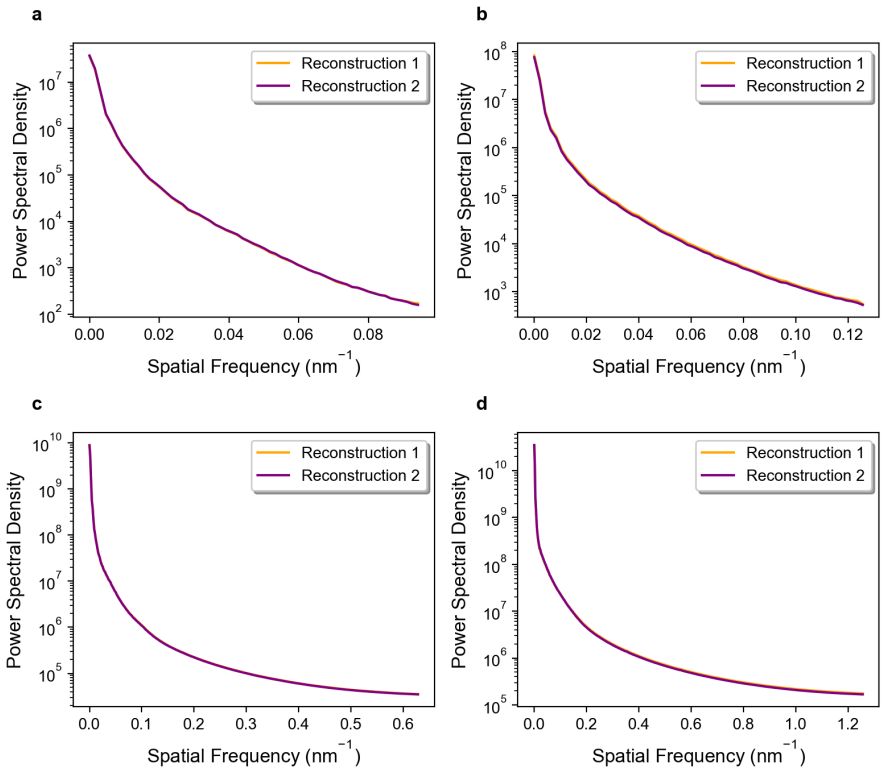

Supplementary Figure 6 | Power Spectral Densities (PSDs) of the 3D XRF images after tomography reconstruction, obtained using two experimental datasets for each sample. **a** PSDs of the obtained low-resolution (LR) 3D XRF images using a Fresnel Zone Plate (FZP). **b** PSDs of the obtained LR 3D XRF images using a pair of Multilayer Laue lenses (MLLs). **c** Corresponding PSDs of the obtained high-resolution (HR) 3D XRF images using FZP. **d** Corresponding PSDs of the HR 3D XRF images using MLLs. When using FZP, the Peak signal-to-noise ratio (PSNR) for LR 3D XRF images is 41.6 dB, and it is 32.7 dB for the corresponding HR 3D XRF images. When using MLLs, the PSNR for LR 3D XRF images is 41.3 dB, and for the corresponding HR 3D XRF image, it is 20.6 dB. The slightly worse performance of the HR 3D XRF image from MLLs compared with FZP is probably due to a relatively large scanning step size. Here, the PSNR for the 3D XRF images is defined as $\mathrm{PSNR} = 20 \times \log_{10}\left(\frac{\mathrm{MAX}}{\mathrm{MSE}}\right)$, where $\mathrm{MSE} = \frac{1}{lmn}\sum_{i=0}^{l-1}\sum_{j=0}^{m-1}\sum_{k=0}^{n-1}[I_1(i,j,k) - I_2(i,j,k)]^2$, and MAX equals to 1. I_1 and I_2 are the corresponding input 3D XRF images.